第3卷 第3期 航空动力学报 Vol.3 No.3
1988年7月 Journal of Aerospace Power July 1988

进口为均匀剪切流的二元亚音扩压器

北京航空航天大学 黄熙君 董金钟 范世兴 肖承恕

摘 要

本文在主流为均匀流的二元亚音扩压器流动计算方法的基础上，发展了一种进口为均匀剪切流的二元亚音扩压器流动特性计算方法。为验证本方法，计算了三种实例，并和试验测定结果进行了比较，二者符合情况良好。

一、 基本方程和计算方法

1. **基本假设：**(1)进口流场存在无粘核心流，具流场为均匀剪切型。(2)扩压器内为定常不可压流。(3)核心主流旋度保持恒定，即沿流向的任一截面上的核心主流保持为均匀剪切流，主流速度分布的斜率保持不变。(4)假设扩压器壁面局部扩张率不大，忽略y向速度分量。

2. **主流方程** 核心流为均匀剪切流，扩压器上、下壁面的主流速度不同。以下标a和b分别表示高、低速侧。根据扩压器连续方程及主流剪切速度分布斜率不变条件，推得：

$$\frac{dU_{an}}{dX_s}=\left(\frac{\lambda-1}{\lambda+1}-\frac{1}{AR^2}\right)\frac{1}{U_{an}}\left(\frac{AR}{Wn}\frac{dWn}{dXs}-\frac{Wn}{1-B_{1a}-B_{1b}}\frac{dBa}{dXs}-\frac{Wn}{1-B_{1a}-B_{1b}}\frac{dB_b}{dX_s}\right)$$

$$\frac{dU_{bn}}{dX_s}=-\left(\frac{\lambda-1}{\lambda+1}+\frac{1}{AR^2}\right)\frac{1}{U_{bn}}\left(\frac{AR}{Wn}\frac{dWn}{dXs}-\frac{Wn}{1-B_{1a}-B_{1b}}\frac{dBa}{dXs}-\frac{Wn}{1-B_{1a}-B_{1b}}\frac{dB_b}{dX_s}\right)$$

式中 $AR=W_n(1-B_a-B_b)/(1-B_{1a}-B_{1b})$， $\lambda=U_{1a}/U_{1b}$， $U_{an}=U_a/U_{1m}$， $U_{1m}=(U_{1a}+U_{1b})/2$， $W_n=W/W_1$， $B_a=\delta_a{}^*/W$， $B_b=\delta_b{}^*/W$。

3. **附面层速度型方程** 为了预估扩压分离流动情况，采用Coles的壁面-尾迹速度分布。引入一些特征参数定义及对x_s求导后可得：

$$dh/dXs=(1.5-0.321V_T{}^2/\Lambda^2)d\Lambda/dX_s+(0.179+0.642V_T/\Lambda)dV_T/dX_s$$

式中 $\Lambda=\delta^*/\delta=V_T+V_B/2, V_T=U\tau/KUe, V_B=2\Pi V_T, h=(H-1)/H=1.5\Lambda+0.179V_T+0.321V_T{}^2/\Lambda$。结合下面将要说明的壁面摩擦关系式经推导可得：

$$dh_a/dX_s=C_{1a}d\Lambda_a/dX_s+C_{2a}dB_a/dX_s+C_{3a}dB_b/dX_s+C_{4a}dW_n/dX_s$$

$$dh_b/dX_s=C_{1b}\Lambda_b/dX_s+C_{2b}dB_b/dX_s+C_{3b}dB_b/dX_s+C_{4b}dW_n/dX_s$$

式中 $C_{1a}=1.5-(3.5-2K_2)V_{Ta}{}^2/\Lambda^2{}_a+C_a(0.115-2\Lambda_a)(0.3+0.4\Lambda_a)R_{ea}{}^{-0.115}/\Lambda_a$

$C_{2a}=0.115V_{Ta}C_a\{[W_n/(1-B_{1a}-B_{1b})][(\lambda-1)/(\lambda+1)-1/AR^2]/U_{an}-1/B_a\}$

$C_{3a}=0.115V_{Ta}C_a[W_n/(1-B_{1a}-B_{1b})][(\lambda-1)/(\lambda+1)-1/AR^2]/U_{an}$

本文于1987年10月收刊。

$C_{4a} = -0.115V_{Ta}C_a\{[(\lambda-1)/(\lambda+1)-1/AR^2]\cdot AR/U_{an}+1\}/W_n$

$C_{1b} = 1.5-(3.5-2K_2)V_{Tb}^2/\Lambda_b^2+(C_b/\Lambda_b)(0.115-2\Lambda_b)(0.3+0.4\Lambda_b)R_{eb}^{*-0.115}$

$C_{2b} = -0.115V_{Tb}C_b[W_n/(1-B_{1a}-B_{1b})]\cdot[(\lambda-1)/(\lambda+1)+1/AR^2]/U_{bn}$

$C_{3b} = 0.115V_{Tb}C_b\{[-W_n/(1-B_{1a}-B_{1b})]\cdot[(\lambda-1)/(\lambda+1)+1/AR^2]\cdot 1/U_{bn}-1/B_b\}$

$C_{4b} = 0.115V_{Tb}C_b\{[(\lambda-1)/(\lambda+1)+1/AR^2]AR/U_{bn}\cdot -1\}/W_n$

$C_a = (2K_2-3)+(7-4K_2)V_{Ta}/\Lambda_a$

$C_b = (2K_2-3)+(7-4K_2)V_{Tb}/\Lambda_b$

$K_2 = 1.589$，$R_e^* = U_e\delta^*/\nu$

4. **壁面摩擦关系式** 文献[1]对壁面摩擦关系式提出：$V_TR_e^*/\Lambda = A[(1-2\Lambda)R_e^*/\Lambda]^N$，对Coles速度型取$A=0.44$，$N=0.886$，得下列摩擦式，并求得上、下壁的摩擦微分式。

$$V_T = 0.44|1-2\Lambda|^{0.866}(\Lambda/R_e^*)^{0.115}\mathrm{Sign}(1-2\Lambda)$$

$$\frac{dV_{Ta}}{dX_s} = \left(\frac{0.115-2\Lambda_a}{1-2\Lambda_a}\right)\frac{V_{Ta}}{\Lambda_a}\frac{d\Lambda_a}{dX_s}-0.115\frac{V_{Ta}}{W_n}\left[1+\left(\frac{\lambda-1}{\lambda+1}-\frac{1}{AR^2}\right)\frac{AR}{U_{an}}\right]\frac{dW_n}{dX_s}+0.115V_{Ta}\left[\frac{W_n}{1-B_{1a}-B_{1b}}\left(\frac{\lambda-1}{\lambda+1}-\frac{1}{AR^2}\right)\frac{1}{U_{an}}-\frac{1}{B_a}\right]\frac{dB_a}{dX_s}+\frac{0.115V_{Ta}}{1-B_{1a}-B_{1b}}\left(\frac{\lambda-1}{\lambda+1}-\frac{1}{AR^2}\right)\frac{W_n}{U_{an}}\frac{dB_b}{dX_s}$$

$$\frac{dV_{Tb}}{dX_s} = \left(\frac{0.115-2\Lambda_b}{1-2\Lambda_b}\right)\frac{V_{Tb}}{\Lambda_b}\frac{d\Lambda_b}{dX_s}-0.115\frac{V_{Tb}}{W_n}\left[1-\left(\frac{\lambda-1}{\lambda+1}+\frac{1}{AR^2}\right)\frac{AR}{U_{bn}}\right]\frac{dW_n}{dX_s}-\frac{0.115V_{Tb}}{1-B_{1a}-B_{1b}}\left(\frac{\lambda-1}{\lambda+1}+\frac{1}{AR^2}\right)\frac{Wn}{U_{bn}}\frac{dB_a}{dX_s}-0.115V_{Tb}\left[\frac{W_n}{1-B_{1a}-B_{1b}}\left(\frac{\lambda-1}{\lambda+1}+\frac{1}{AR^2}\right)\frac{1}{U_{bn}}-\frac{1}{B_b}\right]\frac{dB_b}{dX_s}$$

5. **动量积分方程** 由二元不可压紊流附面层方程导出上、下壁附面层积分方程：

$$A_{11}dB_a/dX_s+A_{12}d\Lambda_a/dX_s+A_{13}dB_b/dX_s+A_{14}d\Lambda_b/dX_s = D_1$$

$$A_{21}dB_a/dX_s+A_{22}d\Lambda_a/dX_s+A_{23}dB_b/dX_s+A_{24}d\Lambda_b/dX_s = D_2$$

式中 $$A_{11} = (1-h_a)W_n-B_aW_nC_{2a}-\frac{B_aW_n^2C_{5a}}{1-B_{1a}-B_{1b}}\left(\frac{\lambda-1}{\lambda+1}-\frac{1}{AR^2}\right)\frac{1}{U_{an}}$$

$$A_{13} = -\left[B_aW_nC_{3a}+\frac{BW_n^2C_{5a}}{1-B_{1a}-B_{1b}}\left(\frac{\lambda-1}{\lambda+1}-\frac{1}{AR^2}\right)\frac{1}{U_{an}}\right]$$

$$D_1 = \frac{C_{fa}}{2}+\left[B_aW_nC_{4a}-B_aC_{5a}\left(\frac{\lambda-1}{\lambda+1}-\frac{1}{AR^2}\right)\frac{AR}{U_{an}}-(1-h_a)B_a\right]\frac{dW_n}{dX_s}$$

$$A_{21} = -\left[B_bW_nC_{2b}-\frac{B_bW_n^2C_{5b}}{1-B_{1a}-B_{1b}}\left(\frac{\lambda-1}{\lambda+1}+\frac{1}{AR^2}\right)\frac{1}{U_{bn}}\right]$$

$$A_{23} = (1-h_b)W_n-B_bW_nC_{3b}-\frac{B_bW_n^2C_{5b}}{1-B_{1a}-B_{1b}}\left(\frac{\lambda+1}{\lambda+1}+\frac{1}{AR^2}\right)\frac{1}{U_{bn}}$$

$A_{12} = -C_{1a}B_aW_n$，$A_{14}=0$，$A_{22}=0$，$A_{24} = -B_bW_bC_{1b}$

$$D_2=\left[B_bW_nC_{4b}+B_bC_{5b}AR\left(\frac{\lambda-1}{\lambda+1}+\frac{1}{AR^2}\right)\frac{1}{U_{bn}}-(1-h_b)B_b\right]\frac{dW_n}{dX_s}-\frac{C_{fb}}{2}$$

$$C_{5a}=3-2h_a+(\zeta_a/\varLambda_a),\qquad C_{5b}=3-2h_b+\zeta_b/\varLambda_b$$

6. **裹入方程**　由裹入率方程可导出：

$$A_{31}dB_a/dX_s+A_{32}d\varLambda_a/dX_s+A_{33}dB_b/dX_s+A_{34}d\varLambda_b/dX_s=D_3$$

$$A_{41}dB_a/dX_s+A_{42}d\varLambda_a/dX_s+A_{43}dB_b/dX_s+A_{44}d\varLambda_b/dX_s=D_4$$

式中

$$A_{31}=\frac{1-\varLambda_a}{\varLambda_a}W_a\left[1-\frac{B_aW_n}{1-B_{1a}-B_{1b}}\left(\frac{\lambda-1}{\lambda+1}-\frac{1}{AR^2}\right)\frac{1}{U_{an}}\right]$$

$$A_{32}=-B_aW_n/\varLambda_a^2,\qquad A_{34}=0,\qquad A_{44}=0$$

$$A_{33}=-\frac{1-\varLambda_a}{\varLambda_a}\ \frac{B_aW_n^2}{1-B_{1a}-B_{1b}}\left(\frac{\lambda-1}{\lambda+1}-\frac{1}{AR^2}\right)\frac{1}{U_{an}}$$

$$D_3=E_a-\frac{1-\varLambda_a}{\varLambda_a}B_a\left[1+\left(\frac{\lambda-1}{\lambda+1}-\frac{1}{AR^2}\right)\frac{1}{U_{an}}\cdot AR\right]\frac{dW_n}{dX_s}$$

$$A_{41}=\frac{1-\varLambda_b}{\varLambda_b}\ \frac{B_bW_n^2}{1-B_{1a}-B_{1b}}\left(\frac{\lambda-1}{\lambda+1}+\frac{1}{AR^2}\right)\frac{1}{U_{bn}}$$

$$A_{43}=\frac{1-\varLambda_b}{\varLambda_b}W_n\left[1+\frac{B_bW_n}{1-B_{1a}-B_{1b}}\left(\frac{\lambda-1}{\lambda+1}+\frac{1}{AR^2}\right)\frac{1}{U_{bn}}\right]$$

$$A_{44}=E_b-\frac{1-\varLambda_b}{\varLambda_b}B_b\left[1-\left(\frac{\lambda-1}{\lambda+1}+\frac{1}{AR^2}\right)\frac{1}{U_{bn}}AR\right]\frac{dW_n}{dX_s}$$

对于裹入率 E，按经验可取为：

$$E=\begin{cases}0.0083(1-\varLambda)^{-2.5} & 0<\varLambda<0.5\\ -0.17+0.438\varLambda & \varLambda>0.5\end{cases}$$

求解：$A\cdot(Z_1,\ Z_2,\ Z_3,\ Z_4)^T=(D_1,\ D_2,\ D_3,\ D_4)^T$

其中　$Z_1=dB_a/dX_s$，$Z_2=d\varLambda_a/dX_s$，$Z_3=dB_b/dX_s$，$Z_4=d\varLambda_b/dX_s$，即可求得扩压器内附面层的参数和主流速度分布。

二、　实验系统

试验是在本院热动力研究所亚音扩压段试验设备[2]上进行的。为模拟进口均匀剪切流条件，在亚音扩压段进口装有可拆装的进口流场模拟装置，试验中采用了多点总压耙测定各扩压截面的总压分布，用壁面静压孔测量各截面静压。

本文试验所采用的模型是一个典型的亚音扩压器。其设计工况为$dMa/dx=0.052$。初始扩压半角为1°53′，局部最大扩张角为8.6°。离试验模型进口50mm处为最小截面。试验和计算均从最小截面作为起始点。试验模型示意图如图1所示。模型全长250mm，宽55mm。

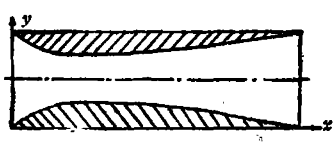

图 1　模型示意图

三、　计算和实验结果的分析比较

在三种不同剪切流型的进口条件下，即进口平均马赫数Ma_1分别为0.31、0.51、和0.56。进口剪切速度比$\overline{\lambda}$为：1.4、1.306和1.2875时，计算出图1扩压器壁面摩擦系数C_f、静压恢

复系数C_p和扩压器上、下壁处主流速度U_e沿扩压器轴线方向的变化规律。计算和实验结果进行了比较（图2～4），符合程度良好。反映出本方法满足工程上对扩压流动特性计算的要求。

图2a给出了$Ma_1=0.31$时C_f分布的计算曲线。由图可见，剪切流在高速壁处C_{fa}下降较慢（曲线A），低速壁处C_{fb}下降较快（曲线B）。$C_{fb}=0$处对应低速壁上附面层分离点。对应回流区，C_{fb}为负值。图中标出了试验测定的分离点s′和计算得出的分离点s，二者吻合良好。图2b是在$Ma_1=0.31$情况下C_p沿扩压器轴向的计算分布曲线，x为实验值。由图可见，分离前后，计算和实验变化规律一致，二者吻合令人满意。这表明本文的方法能够适用于存在分离流动情况下的扩压器特性预估，并能较为完全地反映均匀剪切流的流动特性。

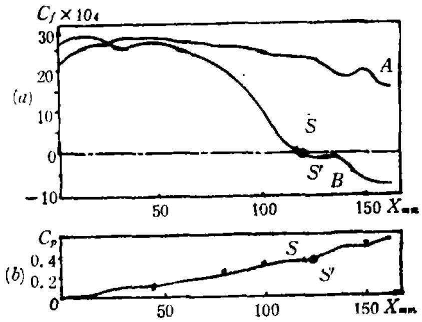

图 2　计算的Cf曲线（a）和Cp的轴向分布（b）($Ma_1=0.31$，$\overline{\lambda}=1.4$)

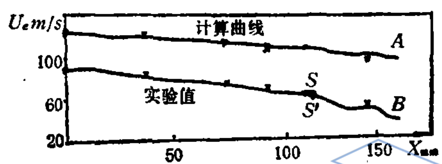

图 3　主流速度Uae和Ueb的分布($Ma_1=0.31$) A、B分别为最高、低速，s为计算分离点，s′为实验分离点

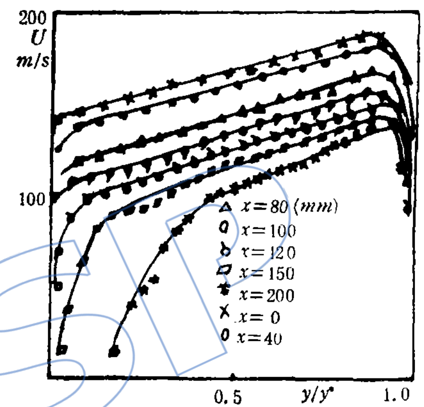

图 4　流速分布测量结果（$Ma_1=0.51$，$\overline{\lambda}=1.306$）

图 3 是在上述进口条件下沿扩压器高、低速壁的主流速度变化特性曲线A和B，x为对应的实验值。计算与实验吻合。说明计算方法中假设主流速度分布斜率沿程不变是符合实际。

图 4 是当$Ma_1=0.51$时沿扩压器的流速分布测量结果。由图可见，均匀剪切主流的速布分布斜率沿流程基本上保持不变。由测量结果可知，高速壁一侧附面层发展不大，低速壁处发展迅速，并存在明显的回流分离区。这与图 2 中摩擦系数变化规律是一致的。

通过上述分析可得如下几点结论：

1．本文所发展的均匀剪切流扩压器流动特性计算方法能正确地预估进口流场为均匀剪切流时的二元亚音扩压器流动特性参数。

2．在均匀剪切主流条件下，扩压器分离通常发生在低速壁一侧。

3．本文所述方法能较为正确地予估扩压器分离点位置，以及分离回流区的壁面摩擦系数和静压恢复系数、预估结果与实验测定结果符合程度良好。

参 考 文 献

〔1〕 Lyrio, A.A., Ferziger, J.H., and Kline, S.T.,"An Integral Method for the Computation of Steady and Unsteady Turbulent Boundary Layer FLows, Including the Transitory Stall Regime in Diffusers", Rpt.PD-23, Thermosciences Div.Mech.Engrg Dept. Stanford University, 1981.

〔2〕 李怀娣、黄熙君、肖承恕、董金钟,"二元扩压器实验研究（二）——不可进口条件下亚音扩压段特性实验研究",北京航空学院科研报告BH-B13461984。

UNSTEADY LOADING NOISE OF COUNTER-ROTATING PROPELLER

Sun Xioafeng, Hu Zongan, Zhou Sheng

(Beijing Institute of Aeronautics and Astronautics)

Abstract

The unsteady Loading noise generated by interaction of a front rotor wake with an aft rotor in a counter-rotating(CR) propeller is analyzed and the noise radiation formulae are derived. The numerical prediction of noise of a real CR propeller are completed and compared with experimental data. It is concluded that the sound pressure level (SPL) in the axial direction of the rotor is fully determined by the component of unsteady loading noise, but in rotor plane the main contribution to SPL is the component of steady loading noise and the effect of the unsteady one is limited in the range of higher harmonics in this case.

TWO-DIMENSIONAL SUBSONIC DIFFUSER FLOW WITH UNIFORM SHEAR VELOCITY PROFILE AT INLET

Huang Xijun, Dong Jinzhong, Fan Shixin, Shio Chengshu

(Beijing Institute of Aeronautics and Astronautics)

A prediction method has been developed for average parameters of 2-D subsonic diffuser with uniform shear velocity profile at inlet. A complete solution of all flow parameters can be obtained by interacting the zonal models and coupling them on common boundaries. The momentum integral and the entrainment equations are used for the boundary layer zone. The equations are closed by use of the improved Cole's wall-wake velocity profile. Due to different development of the boundary layers on the upper and lower walls of diffuser under conditions of the shear velocity profile in core flow, different equations are employed. Three actual diffusers are calculated by this method and experimented by authors. The predictions by this method for the streamwise distribution of pressure coefficient, velocity of core flow and the location of detachment are in good agreement with test data.